做科研，非一朝一夕

买器材，应速战速决

Newport数千种优质产品当日发货，
更多惊喜尽在PhotonSpeed™光速购！

mks | Newport™

Modified frequency-shifted interferometer: encoding wavelength into phase

Xi Chen (陈 希)[1,2,3], Ciming Zhou (周次明)[1], Dian Fan (范 典)[1,*], Li Qian (钱 黎)[1,4], Yandong Pang (庞彦东)[1,2], Cong Wei (魏 聪)[1,2], Chenguang Zhao (赵晨光)[1], Sijing Liang (梁斯靖)[1], and Yuxiao Li (李宇潇)[1,2]

[1]*National Engineering Laboratory for Fiber Optic Sensing Technology, Wuhan University of Technology, Wuhan 430070, China*

[2]*School of Information Engineering, Wuhan University of Technology, Wuhan 430065, China*

[3]*Department of Mechanical and Electrical Engineering, College of Post and Telecommunication, Wuhan Institute of Technology, Wuhan 430073, China*

[4]*Department of Electrical and Computer Engineering, University of Toronto, Toronto, ON M5S 3G4, Canada*

**Corresponding author: fandian@whut.edu.cn*

Received May 13, 2020; accepted June 23, 2020; posted online August 24, 2020

We propose a novel modified frequency-shifted interferometer, where a Mach–Zehnder interferometer is added in order to obtain wavelength information. We use the Hilbert transform to extract the wavelength information from the phase of the interference pattern and construct the relationship between phase and wavelength. The laser wavelength measurement experiment is used to verify the compound interferometer. Experimental results demonstrated that our method could obtain the wavelength from the phase, which is of great significance for demodulation of the fiber Bragg grating based on a frequency-shifted interferometer.

Keywords: modified frequency-shifted interferometry; phase difference; Hilbert transform.
doi: 10.3788/COL202018.101203.

Recently, the frequency-shifted interferometer (FSI) has been studied and applied to fiber-optic sensor sensing, which attracts the interest of many researchers[1–11]. FSI utilizes a frequency shifter [usually, an acoustic optic modulator (AOM)] asymmetrically inserted in a Sagnac loop, producing location-resolved information for multiple sensors without resorting to wavelength-division or time-division multiplexing. Since the Sagnac interferometer is self-referenced, no coherence requirement is needed for the light source. FSI also results in a high signal-to-noise ratio (SNR) and does not require a fast detector[9]. However, the interference signal of FSI does not contain wavelength information of the light reflected from the sensor. If we need to obtain wavelength information, it is necessary to use either a tunable laser source or a tunable filter to scan the optical wavelength, which causes more complexity and adds to the cost.

In this Letter, we propose a novel modified FSI (MFSI) based on a compound interferometer structure to address the above problems. We modified the optical path structure, adding a Mach–Zehnder interferometer (MZI) in the conventional FSI, forming a compound interferometer. Two counter-propagating light waves go through different paths and encode wavelength information into the phase of the interference signal. We adopt the Hilbert transform (HT) to convert the phase into a wavelength[12–14]. We calibrate the system with a laser source of known wavelength to establish the relationship between the initial phase of the interference signal and this known wavelength. Thereafter, the unknown wavelength can be calculated from the initial phase. Here, we demonstrate only the capability of extracting wavelength information, without sensors in the MFSI. Our method is tested with interference signals obtained from the MFSI system, the results show it is feasible, simple, and with low cost, and it is vital to extend the applications of FSI.

The schematic diagram of the MFSI based on the compound interferometer is depicted in Fig. 1.

A 50/50 fiber coupler C_1, path A, and path B constitute a Sagnac loop, and an AOM in path B acts as a frequency shifter. An MZI is formed by a circulator (CIR-2) and a 50/50 fiber coupler C_2 (included in path A), with slightly different path lengths L_b and L_c. The phase difference (PD) between path L_b and L_c is a function of wavelength, and therefore the wavelength information can be extracted from this PD. A polarization controller (PC) is employed to improve the interference visibility.

After passing through CIR-1, the light signal is split equally at C_1 and input in the clockwise (CW) and counterclockwise (CCW) directions. Then, upon returning to C_1, each time light passes through the AOM, and its frequency is up-shifted by an amount equal to the frequency of the acoustic driving signal f. The intensity signal ΔI at the balanced detector (BD) is[8,15]

$$\Delta I = A \sin\left[\frac{2\pi n(\lambda)L}{c} f - \frac{2\pi n(\lambda)}{\lambda}\Delta L\right], \tag{1}$$

$$A = -4\kappa_A\kappa_B(1-\gamma_1)(1-\gamma_2)\gamma_2\gamma_1 E_0^2, \tag{2}$$

where A is the transmission coefficient, κ_A and κ_B are the transmission coefficients of path A and path B, γ_1 and γ_2

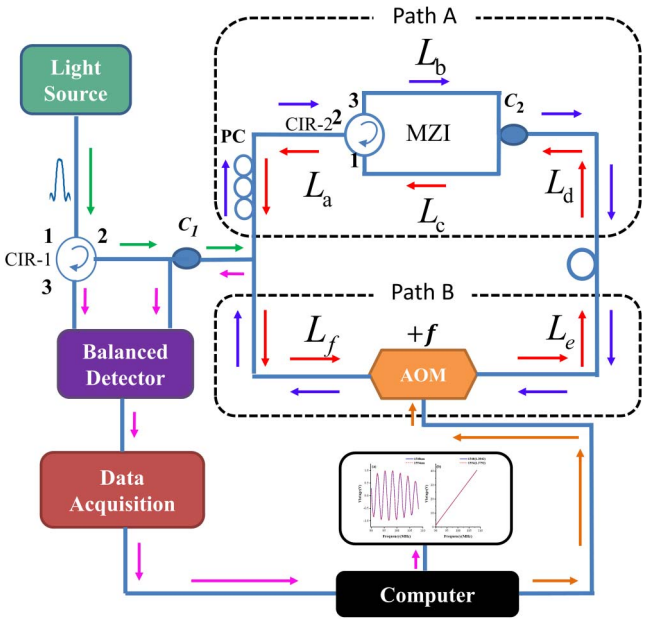

Fig. 1. Schematic diagram of the MFSI based on a compound interferometer. AOM, acoustic optic modulator; CIR-1, CIR-2, circulators; PC, polarization controller; C_1, C_2, fiber couplers; MZI, formed by CIR-2 and C_2.

are the coupling ratios of C_1 and C_2, λ is the wavelength of the light source, E_0 is the input field amplitude, $n(\lambda)$ is the refractive index of the fiber which, considering dispersion, is a function of wavelength, c is the speed of light in vacuum, f is the amount of frequency shift caused by the AOM, $\Delta L = L_b - L_c$ is the length difference of path A, $L = (L_a + L_c + L_d + L_e - L_f)$ is a constant, L_a, L_b, L_c, L_d, L_e, and L_f are the fiber lengths in Fig. 1. In Eq. (1), the differential output ΔI is a sine function of f when we sweep the frequency of the frequency shifter linearly, f changes with time, and ΔI is a sine function changing with time t.

From Eq. (1), the initial phase (when $f = f_o$) is a function of wavelength. In signal processing, HT is used to construct an analytic signal, which can calculate envelope (instantaneous amplitude) and instantaneous phase. Therefore, we use HT to extract the wavelength from the initial phase.

Suppose $x(t)$ is the real signal corresponding to Eq. (1); using HT, it can be converted to an analytic sequence: $Z(\mathrm{t}) = x(t) + j\bar{x}(t)$, where $\bar{x}(t)$ is the HT of $x(t)$. The instantaneous phase can be expressed as

$$\phi(t) = \arctan\left[\frac{\bar{x}(t)}{x(t)}\right]. \tag{3}$$

Combined with Eq. (1), it can also be expressed as

$$\phi(t) = \frac{2\pi n(\lambda) L}{c} f - \frac{2\pi n(\lambda)}{\lambda}\Delta L. \tag{4}$$

As described in Eq. (4), the frequency f is a function of time, and there is a unique single value of the instantaneous phase at any given time measured in radians. It would oscillate between $-\pi$ and π because of the periodicity of the arctangent function. After unwrapping the instantaneous phase and fitting it to a line, it can be seen that the slope of the line is $2\pi n(\lambda)L/c$, and the intercept is $-2\pi n(\lambda)\Delta L/\lambda$, which contains the wavelength of the light source. By calculating the instantaneous phase intercept of HT, we can get the initial phase including the wavelength. If there is another light source with a wavelength of λ', to calculate their initial PD, we can get the following expression as

$$\Delta\phi(t) = -2\pi\Delta L\left[\frac{n(\lambda)}{\lambda} - \frac{n(\lambda')}{\lambda'}\right]. \tag{5}$$

Suppose $\lambda' = \lambda + \Delta\lambda$, using Taylor expansion, then

$$n(\lambda') = n(\lambda) + \frac{\mathrm{d}n}{\mathrm{d}\lambda}\Delta\lambda, \tag{6}$$

and $\Delta\phi(t)$ can also be expressed as

$$\Delta\phi(t) = \frac{-2\pi\Delta L}{\lambda}\left[\frac{n(\lambda)}{\lambda} - \frac{\mathrm{d}n}{\mathrm{d}\lambda}\right]\Delta\lambda. \tag{7}$$

In Eq. (6), there is a corresponding relationship between the PD and the wavelength difference of two interference signals with different wavelengths, and it is related to ΔL. Keeping ΔL very short and temperature stabilized, ΔL can be considered as a constant. Hence, the relationship between PD and wavelength difference can also be considered stable. Therefore, we can take this relationship and the initial phase of a known wavelength as the initial parameters of the laser measurement system. By using the light source with known wavelength to calibrate the system, the initial phase of the known wavelength and the relationship between the wavelength difference and the PD can be obtained. Due to the periodicity of phase, the interference signals of two different wavelengths with a PD of 2π will coincide. So, we can use this feature to calibrate the system.

The calibration process is as follows.

1. Set an initial wavelength through the light source with known wavelength and record the interference signal and initial phase.
2. Adjust the wavelength of the light source and observe the interference signal until it coincides with the interference signal obtained with the initial known wavelength.
3. Repeat step 2 and obtain the wavelength differences between successive coincidences of the interference signal (corresponding to 2π phase change), thereby obtaining the relationship between wavelength difference and PD.
4. Set this relationship and the values of the initial wavelength and the initial phase as the initial measurement parameters.

After calibration, the initial parameters can be treated as constants. Then, we can measure the unknown wavelength through its initial phase and initial parameters.

The experimental setup is depicted in Fig. 1. The output power of tunable semiconductor laser (TSL) (Santec TSL-510) is set to 2 mW. The AOM (Brimrose AMM-100-20-25-1550-2FP) is swept from 90 to 110 MHz at steps of 0.02 MHz with a step time interval of 1 ms. The output of the BD (New Focus Model 2117) was sent to a data acquisition board (NI USB-6361) with a sampling rate of 100 kHz and synchronized with the AOM scanning cycle. The gain of the BD is set to 10^3, with a corresponding bandwidth of 100 kHz. The optical backscatter reflectometer (OBR) (LUNA OBR4600) was used to make an MZI of path A, and it measured L_b and L_c. The ΔL is calculated as -1.6×10^{-4} m, which means L_b is less than L_c.

A LabVIEW program was developed and used to control the AOM frequency sweep and to acquire and process the data by the computer.

The grating sensors in our laboratory are most concentrated on the wavelength range starting from 1548 nm, in order to facilitate the research of MFSI in the future; the free spectral range (FSR) of the measurement system starts from the wavelength of 1548 nm.

At the beginning of calibration, FSR was larger than 6 nm. However, ΔL is affected by fiber attitude and ambient temperature, resulting in FSR changing unsteadily. In order to obtain a stable FSR, we adjusted the fiber attitude in a relatively stable environment at room temperature and observed the period through the TSL. During adjusting, there may be some stretching of L_b or L_c, causing FSR to change to around 6 nm. Considering the situation of the experimental equipment and the convenience of calculation, we choose to adjust the FSR to 6 nm and keep it stable. In Fig. 2(a), we show the interference signal obtained for the AOM sweep range of 90–110 MHz for two different wavelengths. (Note, data in the small region near the end of the range is removed due to instability in AOM sweeping.) We set 1548 nm as the initial wavelength for calibration. The calibration results are shown in Fig. 2(b).

In Fig. 2(a), as can be seen, the interference signals at the 1548 nm and 1554 nm wavelengths have almost overlapped; according to the periodic characteristic of phase 2π and the method of system calibration, when the wavelengths of 1548 nm and 1554 nm coincide for the first time, it clearly illustrates that the wavelength difference of 6 nm corresponds to the PD of 2π. According to the results and Eq. (5), if the refractive index does not change with the wavelength, the value is assumed to be 1.468. ΔL can be calculated as 2.731×10^{-4} m. Figure 2(b) shows their phase intercept.

After obtaining the corresponding relationship between the PD and wavelength difference, we saved the interference data to test our method on the actual signal processing and selected the interference data with TSL wavelength sweeping from 1548 nm to 1554 nm.

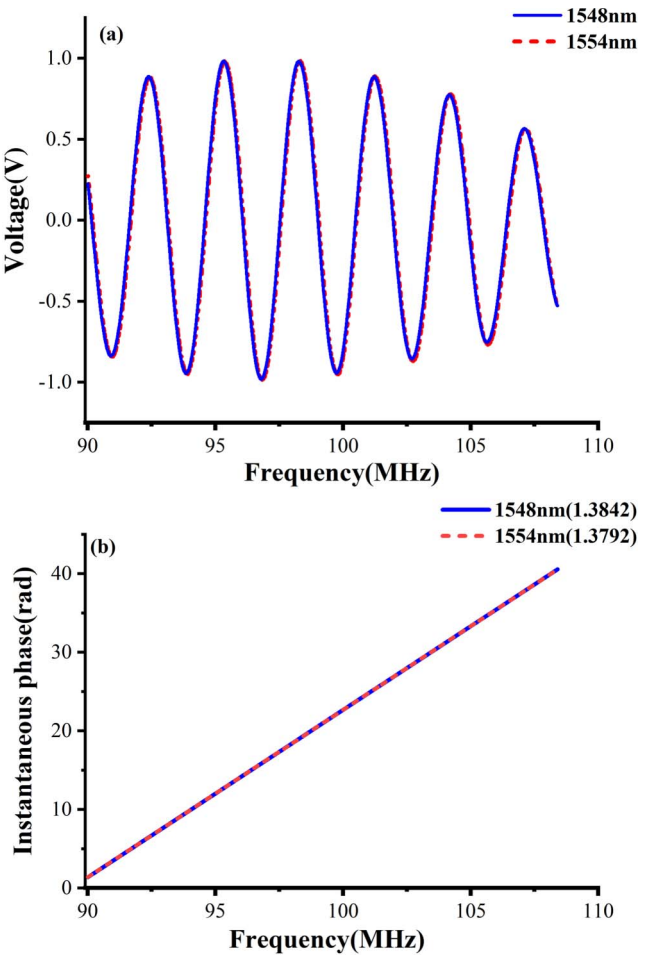

Fig. 2. (a) Interference signal from MFSI obtained at 1548 nm and 1554 nm and (b) 1548 nm and 1554 nm phase intercept.

Figure 3(a) shows the 1548 nm to 1553 nm interference signal changes. Figure 3(b) shows their phase changes at the initial phase. Combined with Fig. 2, the initial parameter of the wavelength is set as 1548 nm, and the PD and the measured wavelength (MWL) are shown in Table 1.

It can be seen from Table 1 that when the wavelength of TSL increases, the initial phase value gradually decreases. The phase of 1554 nm is similar to the phase of 1548 nm. It can be inferred that the FSR of our measurement system is 6 nm. The little bit of inconsistency between 1548 nm and 1554 nm may be caused by the system noise and other factors affecting ΔL. Moreover, there is a mutation in the phase of 1553 nm; by subtracting 2π from the abrupt change of phase, the continuous change of phase can be ensured, which means that, for the unknown wavelength measurement, the wavelength measurement range is only the FSR. In addition, from the theoretical analysis and experiment test results, it is also known that the calculation of the phase demodulation wavelength using the arctangent function will produce periodic multi-values, that is, phase ambiguity[16]. Although we use the unwrapped function of MATLAB to solve the phase, the intercept is still limited between $-\pi$ and π, which caused one initial phase to correspond to multiple different wavelengths

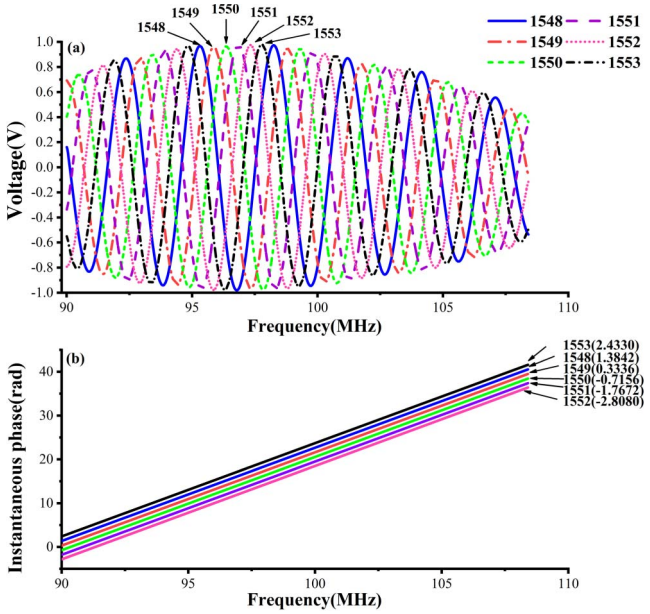

Fig. 3. Wavelength 1548–1553 nm interference signal and their phase changes intercept. (a) Wavelength 1548–1553 nm interference signal and (b) 1548–1553 nm phase changes intercept.

Table 1. Results of the Experiment

TSL (nm)	Phase (rad)	PD (rad)	MWL (nm)
1548.000	1.3842	0.0000	1548.000
1549.000	0.3336	−1.0506	1549.003
1550.000	−0.7156	−2.0998	1550.005
1551.000	−1.7672	−3.1514	1551.009
1552.000	−2.8080	−4.1922	1552.004
1553.000	2.4330	−5.2343	1552.999
1554.000	1.3792	−0.0050	1548.005

(e.g., 1548 nm or 1554 nm), thus limiting the measurement range of our system to the FSR of 6 nm. To solve the phase ambiguity problem, we can extend the phase ambiguity boundary by shortening ΔL. Also, to improve the accuracy, we can maintain the ΔL stability.

We presented and demonstrated a novel MFSI based on the compound interferometer to obtain the wavelength of the light source. The wavelength information is converted into the interference phase by embedding an MZI in a conventional FSI. The laser wavelength measurement experiment is used to verify the compound interferometer. The absolute measurement of laser wavelength can be realized by using the known wavelength and the PD of the detection interference signal. The experiment results show that our MFSI system does not need a reference laser for the scanning wavelength, which can lower the cost and is of great significance for demodulation FBGs based on FSI.

This work was supported by the National Natural Science Foundation of China (NSFC) (Nos. 61775173 and 61975157). The authors thank Miao Gao with the School of Mechanical Engineering in the Wuhan Vocational College of Software and Engineering for her valuable support on paper writing. The authors also thank Yuan Ma with GTL Technology & Service Co., Ltd. for his meaningful help with making the MZI and measuring ΔL.

References

1. B. Qi, A. Tausz, L. Qian, and H. K. Lo, Opt. Lett. **30**, 3287 (2006).
2. Q. Bing, L. Qian, A. Tausz, and H.-K. Lo, IEEE Photon. Technol. Lett. **18**, 295 (2006).
3. Y. Fei, Q. Li, and Q. Bing, in *Conference on Optical Fiber Communication/National Fiber Optic Engineers Conference IEEE* (2008), p. 1.
4. F. Ye, L. Qian, Y. Liu, and B. Qi, IEEE Photon. Technol. Lett. **20**, 1488 (2008).
5. F. Ye, T. Chen, D. Xu, K. P. Chen, B. Qi, and L. Qian, Appl. Opt. **49**, 4898 (2010).
6. F. Ye, B. Qi, and L. Qian, Opt. Lett. **36**, 2080 (2011).
7. H. Tian, C. M. Zhou, D. Fan, Y. W. Ou, and D. J. Yin, Chin. Opt. Lett. **12**, 120604 (2014).
8. F. Ye, Y. Zhang, B. Qi, and L. Qian, Sensors (Basel) **14**, 10977 (2014).
9. Y. W. Ou, C. M. Zhou, L. Qian, D. Fan, C. F. Cheng, and H. Y. Guo, Opt. Express **23**, 31484 (2015).
10. Y. W. Ou, C. M. Zhou, L. Qian, D. Fan, C. F. Cheng, H. Y. Guo, and Z. Xiong, IEEE Photon. Technol. Lett. **29**, 535 (2017).
11. X. Gui, M. A. Galle, L. Qian, W. Liang, C. Zhou, Y. Ou, and D. Fan, Chin. Opt. Lett. **16**, 010606 (2018).
12. D. Huang, J. Zhao, and J. Su, Acta Oceanolog. Sin. **22**, 1 (2003).
13. M. Feldman, Mech. Syst. Sig. Process. **25**, 735 (2011).
14. Y. L. Shen, Y. Q. Tu, L. J. Chen, and T. A. Shen, Meas. Sci. Technol. **26**, 095003 (2015).
15. J. Miao, X. Zhang, Z. Li, Z. Cui, Y. Zhang, D. Liu, and J. Zhu, Chin. Opt. Lett. **16**, 061201 (2018).
16. Y. Li and L. Ma, Inf. Laser Eng. **44**, 2800 (2015).